MOLECULAR AND CELLULAR BIOLOGY, Oct. 2010, p. 4595–4603 Vol. 30, No. 19
0270-7306/10/$12.00 doi:10.1128/MCB.01618-09

Renal Oxygenation Suppresses VHL Loss-Induced Senescence That Is Caused by Increased Sensitivity to Oxidative Stress▽†

Scott M. Welford,[1,2] Mary Jo Dorie,[1] Xiaofeng Li,[2] Volker H. Haase,[3] and Amato J. Giaccia[1]*

Department of Radiation Oncology, Stanford University School of Medicine, Stanford, California 94305[1]; Department of Radiation Oncology, Case Western Reserve University, Cleveland, Ohio 44106[2]; and Departments of Medicine, Cancer Biology, Molecular Physiology, and Biophysics, Vanderbilt University School of Medicine, Nashville, Tennessee 37232[3]

Received 16 December 2009/Returned for modification 16 March 2010/Accepted 6 July 2010

Loss of the VHL tumor suppressor is regarded as an initiating event in the development of clear-cell renal carcinoma. Surprisingly, loss of VHL induces senescence in mouse fibroblasts *in vitro*, a response that would restrict development of renal carcinoma *in vivo*. Typical *in vitro* cell culture levels of oxygen, however, are significantly higher than physiological levels of oxygen, which have been shown to abrogate senescence induced by many stimuli. Therefore, we investigated the oxygen dependence of VHL loss-induced senescence. Using mouse fibroblasts and primary renal epithelial cells *in vitro*, we found that VHL loss leads to senescence under atmospheric conditions (21% O_2), partly through increasing p27 levels, but not under physiological oxygenation (2% to 5% O_2), despite maintaining increased p27 expression. This suggests that VHL inactivation sensitizes cells to oxidative stress. In support of this concept, senescence following VHL loss depends on p53 activity, which decreases under the less stressful conditions of mild hypoxia. We confirmed these observations *in vivo* by treating kidney-specific VHL knockout animals with the potent oxidizer paraquat and observed a robust induction of cellular senescence. Together, these data demonstrate that *in vivo* oxygenation promotes tolerance of VHL loss in renal epithelia, which may promote the development of renal carcinoma.

Mutation of the *VHL* gene is associated with the hereditary cancer syndrome von Hippel-Lindau disease, which is characterized by central nervous system (CNS) and retinal hemangioblastomas, pheochromocytomas, and clear-cell renal cell carcinomas (CCRCC). *VHL* is a tumor suppressor that follows the Knudson "two-hit" model, whereby individuals inherit a mutant allele and then acquire a second, somatically inactivated copy during their lifetimes. Sporadic development of CCRCC is also associated with inactivation of *VHL* in a majority of cases.

The best-studied role of VHL is in oxygen sensing (16). VHL is a critical component of a ubiquitin-conjugating complex that targets the heterodimeric hypoxia-inducible factors (HIF) for degradation under aerobic conditions. Oxygen-dependent posttranslational modification of the HIFα subunits allows association with VHL and subsequent degradation. Under hypoxic conditions, or in the absence of VHL, the HIF transcription complexes are stabilized and activated and lead to the transcription of a diverse set of target genes that are broadly involved in adaptation to low-oxygen conditions. Interestingly, many of these genes have also been linked to protumorigenic functions, including angiogenesis, glycolysis, survival, and metastasis (3).

In addition to regulating adaptation to hypoxia, VHL has also been implicated in the maintenance of primary cilia, microtubule stability, and regulation of the extracellular matrix. It is unclear if these functions are specifically linked to tumorigenesis; however, they are likely to contribute to many of the other clinical manifestations of VHL disease (15). In addition, loss of VHL has recently been demonstrated to induce senescence in mouse embryo fibroblasts (MEFs) (41). This observation contributes to an increasingly prevalent theme of oncogene activity or tumor suppressor loss in primary cells, leading to senescence to act as a barrier to malignant progression (4, 6, 22, 33).

Senescence plays a critical role in tumor suppression. It can result from telomere shortening, oncogene expression/tumor suppressor loss, or adverse culture conditions. Interestingly, senescence is influenced significantly by oxidative stress: oxidizing agents induce senescence while reducing agents inhibit senescence. Moreover, senescence can be inhibited by culturing cells in low-oxygen environments (17, 25, 26). Indeed, under atmospheric oxygen tensions (21% O_2, commonly referred to as "normoxia"), wild-type or oncogene-expressing MEFs display a limited growth potential that culminates in senescence, while under low-oxygen conditions (2 to 3% O_2), cells proliferate indefinitely. This increased growth potential is partly due to reduced oxidative stress under low partial O_2 pressure (pO_2) and partly to increased tolerance for such stress (26, 38). Given that normal physiological oxygen concentrations range from as high as 14% in the lungs to 1 to 2% in parts of the brain, heart, and skin (35), these observations suggest that what induces senescence in atmospheric oxygen *in vitro* may or may not represent normal cellular responses *in vivo*.

In the kidney, oxygen ranges from 1.5% in the inner medulla to 7% in the outer cortex (1, 18), levels that are often sufficient to alleviate the onset of senescence. As mutation of *VHL* has been found to be one of the earliest lesions in the development of CCRCC (21), we sought to investigate how the loss of VHL

* Corresponding author. Mailing address: Department of Radiation Oncology, Stanford University School of Medicine, 1235 CCSR, 269 Campus Drive, Stanford, CA 93025. Phone: (650) 723-7311. Fax: (650) 723-7382. E-mail: giaccia@stanford.edu.

† Supplemental material for this article may be found at http://mcb.asm.org/.

▽ Published ahead of print on 2 August 2010.

would be tolerated under physiological conditions and, in particular, in renal epithelial cells, where VHL mutations occur. Understanding how these cells react to VHL loss is critical to determining the etiology of the disease.

MATERIALS AND METHODS

Cell culture. $VHL^{f/f}$ and $VHL^{f/f}$ HIF-$2\alpha^{f/f}$ MEFs were harvested as described previously (38). For each experiment, MEFs were thawed and manipulated in 2% O_2 in a Ruskinn In Vivo$_2$ Hypoxia Work Station before being subjected to appropriate pO_2 in like chambers. Gamma irradiation was carried out with an open-source ^{137}Cs irradiator. H_2O_2 treatments were performed with cells at confluence to reduce H_2O_2 toxicity; the cells were plated 24 h later and followed for markers of senescence. Proteasome inhibition was effected by 10 μM MG132 for 8 h. For synchronization, MEFs were cultured in Dulbecco's modified Eagle's medium (DMEM) plus 0.1% serum for 72 h and stimulated with 20% serum for the indicated times. Cells were analyzed for propidium iodide staining using standard procedures. Doxorubicin treatment was 0.2 μg/ml for 5 h. Adenoviral infections were carried out as described previously (38). Primary renal tubule epithelial cells (PTECs) were harvested as described previously (34) and plated directly in the indicated pO_2. All short hairpin RNAs (shRNAs) were in pLKO.1 from Open Biosystems (shp27, clone TRCN0000071067; shHIF-1α, clone TRCN0000054448; and shp53, GTACTCTCCTCCCCTCAAT).

Proliferation, senescence, and comet assays. Proliferation assays and senescence staining were performed as described previously (7, 38). Alkaline comet assays were also described previously (8). Error bars throughout indicate standard deviations. Unpaired two-tailed Student's *t* tests were performed to determine significance.

Northern and Western blotting and immunofluorescence. Northern and Western blotting were performed using standard procedures. Where applicable, cell lysates were harvested in the hypoxia chambers without reoxygenating the cells. The antibodies used were as follows: HIF-1α, Bethyl A300-286A; p27, Transduction Labs K25202; β-actin, Santa Cruz sc1615; cyclin A, Santa Cruz sc-596; cyclin D1, Cell Signaling DCS6; cyclin E, Upstate Biosystems 06459; p21, Santa Cruz sc-756; aryl hydrocarbon receptor nuclear translocator (ARNT), Transduction Labs 611079; p53, Santa Cruz sc-126; p53Ser15, Cell Signaling 9284; γH2AX, Cell Signaling 9718; and tubulin, RDI Tubulaadm-DM. β-actin, tubulin, and ARNT were used as loading controls. For immunofluorescence, the following antibodies were used: fluorescein isothiocyanate (FITC)-conjugated α-pimonidazole (Chemicon 90531) and Glut1 (Thermo Scientific RB-9052P). The lectins used were rhodamine-conjugated peanut agglutinin (Vector Labs RL-1072) and fluorescein-conjugated *Griffonia simplicifolia* lectin II (Vector Labs FL-1211). For pimonidazole staining, animals were injected with 60 mg of Hypoxyprobe-1 (NPI, Inc.)/kg of body weight 90 min before being sacrificed.

PCR and QRT-PCR. Primers for genotyping the $VHL^{f/f}$ animals have been previously described (11). The *CRE* genotyping primers were TGGGCGGCAT GGTGCAAGTT and CGGTGCTAACCAGCGTTTTC. Quantitative real-time PCR (QRT-PCR) was performed on an ABI7900HT using *Power* SYBR green Master Mix and following standard procedures. The primer sequences were as follows: *Vhlh*, CAGCTACCGAGGTCATCTTTG and CTGTCCATCGACATT GAGGGA; *Glut1*, CAGTTCGGCTATAACACTGGTG and GCCAGAGGGG TTTCTGTCG.

Animal studies. PEPCK-CRE VHL animals have been described previously (29). Animals of appropriate genotypes were treated with 10 mg/kg paraquat dichloride by intraperitoneal (i.p.) injection two times 1 week apart. The animals were sacrificed 4 weeks after the initial treatment, and their kidneys were sunk in 30% sucrose/1× phosphate-buffered saline (PBS) overnight, frozen in optimal cutting temperature compound (OCT), and sectioned. The sections were stained for senescence-associated beta-galactosidase activity (SA-β-Gal) as described previously (7). Immunohistochemistry for Glut-1 and DcR2 (Stressgen) was performed using standard procedures.

RESULTS

Loss of VHL induces senescence in an oxygen-dependent manner. In order to determine the oxygen dependence of VHL loss-induced senescence, we used MEFs derived from a conditional *Vhlh loxP* mouse (11) and excised the *Vhlh* gene using an adenovirus that expresses *cis*-acting replication element (CRE) recombinase (Adeno-CRE). VHL expression was reduced by roughly 85% as measured by quantitative real-time PCR (Fig. 1A), and the levels of Glut1, encoded by a classic HIF-1α target gene, increased 6-fold in the Adeno-CRE-infected cells ("VHL null") compared to adenovirus-infected control cells (wild type ["wt"]). Under progressively lower oxygen concentrations, Glut1 levels in the control cells increased with activation of the HIF pathway and stabilization of HIF-1α (Fig. 1B).

We next monitored the proliferation of these cells grown at 21%, 10%, 5%, and 2% O_2 over a 3-week period. Importantly, all manipulations of cells (for these and all subsequent experiments unless otherwise noted) prior to the start of the growth assays were performed under 2% O_2, a condition that preserves the replication potential of the cells (26). Under 21% O_2, wild-type MEFs continued to divide for 2 weeks before succumbing to stress-induced senescence (Fig. 1C, upper left). As noted above, loss of VHL led to rapid arrest and failure to proliferate. By day 12 of the assay, both populations of cells demonstrated classic signs of senescence, including flattened cellular morphology and positivity for SA-β-Gal (Fig. 1D; see Fig. S1 in the supplemental material). Notably, the VHL-null cells demonstrated significantly more SA-β-Gal-positive cells than the wild-type cells (55.2% ± 12.0% versus 21.2% ± 8.3%, respectively) owing to their earlier entrance into the senescent state.

At 10% O_2, wild-type cells displayed a significant growth advantage over wild-type cells grown at 21% O_2 and over VHL-null cells grown at 10% O_2, continuing to proliferate without entering senescence (Fig. 1C, upper right). The VHL-null cells proliferated more than at 21% O_2 but still arrested and became SA-β-Gal positive (Fig. 1D; see Fig. S1 in the supplemental material). In stark contrast, both wild-type and VHL-null cells proliferated continuously at both 5% and 2% O_2 (Fig. 1C, bottom). Neither population entered senescence as measured by proliferation, morphology, or SA-β-Gal staining. Thus, these data confirm that VHL inactivation leads to senescence but demonstrate that it does so in an oxygen-dependent manner.

VHL loss sensitizes cells to oxidative stress. High oxygen levels are associated with high levels of oxidative stress, the cumulative effects of which result in the induction of senescence (10, 37). This is a graded effect, dependent on the amount of stress and the length of exposure (26). To determine if senescence due to VHL loss is dependent on continuous exposure to high oxygen levels, we next asked whether we could rescue VHL loss-induced senescence by returning cells to a low-oxygen environment after exposure to 21% for various periods of time. This proved to be the case, but only up to a certain point before the accumulated stress of hyperoxia was irreversible (Fig. 2A to C). Cells that were moved to 5% oxygen after a 4-day exposure to 21% oxygen recovered rapidly and evaded senescence similarly to cells grown continuously at 5% oxygen. Cells that experienced 8 days at 21% O_2 recovered less well, and cells that were at 21% O_2 for 12 days hardly recovered at all. Thus, continuous exposure to high oxygen levels is necessary for VHL deficiency to induce senescence. Since both wild-type and VHL-null cells eventually senesce under these conditions but VHL-null cells do so at an increased rate, this observation suggests that VHL-deficient cells

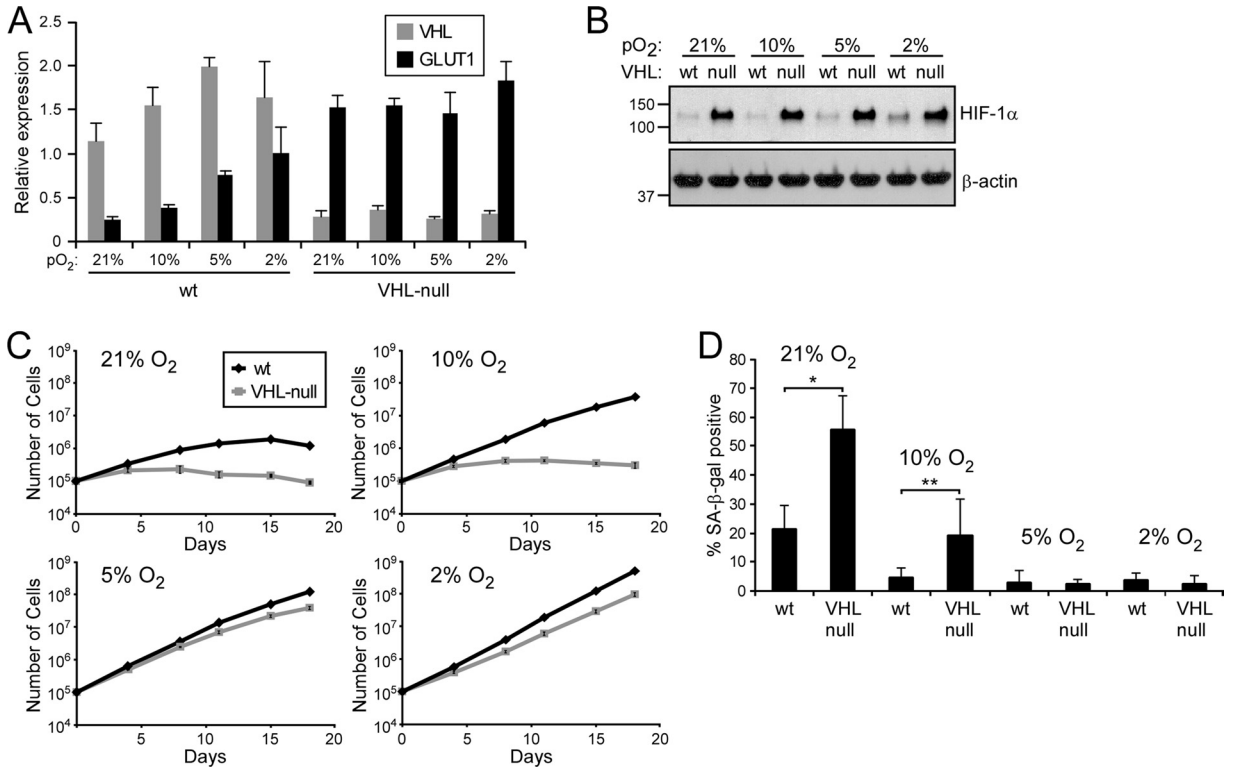

FIG. 1. VHL loss induces senescence in an oxygen-dependent manner. (A) QRT-PCR analysis of wild-type (wt) and VHL-null MEFs grown at various levels of pO_2. (B) Western analysis of protein harvested from the cells described in panel A. (C) Proliferation profiles of the cells described in panel A. (D) Quantification of SA-β-Gal staining of cells in panel C at day 12 (*, $P = 0.017$; **, $P = 0.046$). The error bars represent standard deviations.

have an increased sensitivity to oxidative stress that leads to premature senescence.

To test this hypothesis, we exposed wild-type and VHL-deficient cells that were grown at lower oxygen levels (5% O_2) to various doses of ionizing radiation (IR) or H_2O_2, both of which cause robust oxidative stress through the production of oxygen radicals (10), and then monitored the induction of senescence 8 to 12 days later. Indeed, the VHL-null cells en-

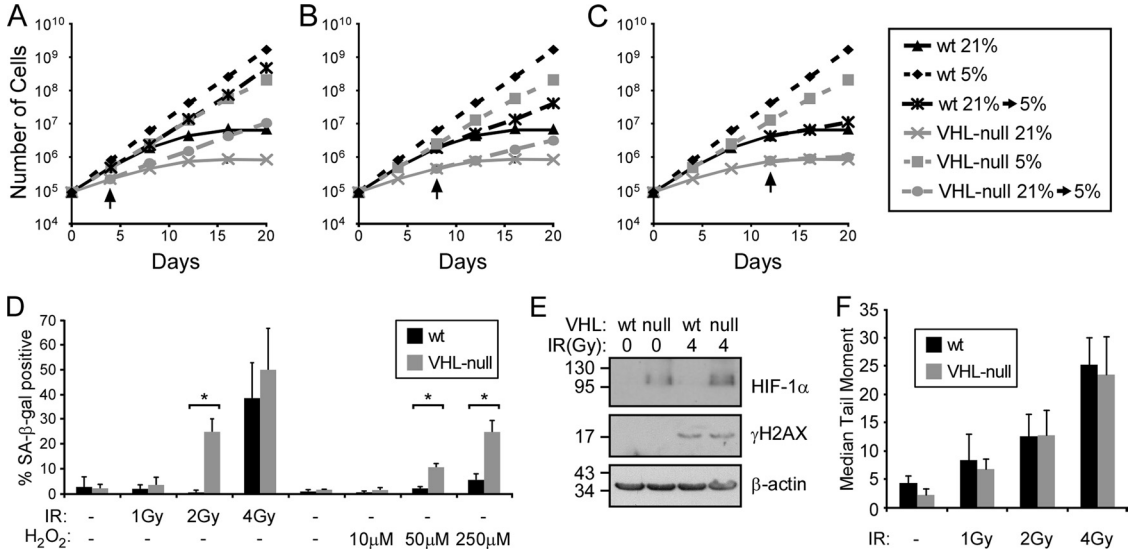

FIG. 2. VHL loss sensitizes cells to oxidative stress. (A to C) Growth assays of wild-type and VHL-null MEFs grown at 21% oxygen or 5% oxygen or grown for 4 days (A), 8 days (B), or 12 days (C) at 21% oxygen before being moved to 5% oxygen. The arrows indicate when the cells were transferred to 5% oxygen. (D) Quantification of SA-β-Gal staining of cells grown at 5% O_2 12 days after treatment with various doses of ionizing radiation (*, $P < 0.001$), or treated with H_2O_2 and assayed after 8 days. (E) Western blot analysis of wild-type and VHL-null cells before and 30 min after 4 Gy of IR for γH2AX staining. (F) Quantification of the median tail moments of nuclei in denaturing comet assays with or without IR treatment, as indicated. The error bars represent standard deviations.

tered senescence at a lower dose of IR or H_2O_2 than did the wild-type cells (Fig. 2D; see Fig. S2 and S3 in the supplemental material). Two gray of IR resulted in 25.1% (±5.2%) of the cells staining for SA-β-Gal while it did not affect the wild-type cells. At 4 Gy, 56.7% (±2.8%) of the VHL-null and 38.6% (±1.4%) of the wild-type cells became SA-β-Gal positive. Likewise, in response to H_2O_2, 10.8% (±1.5%) of VHL-null cells, but only 2.3% (±0.07%) of wild-type cells, became senescent at 10 μM, and 25.0% (±4.63%) of the VHL-null versus 5.7% (±2.5%) of the control cells were senescent at 250 μM. Together, these data demonstrate that VHL loss leads to increased sensitivity to oxidative stress that causes VHL-deficient cells to enter senescence at a lower level of stress than wild-type cells.

VHL deficiency does not lead to higher basal levels of DNA damage. Oxidative stress has been shown to provoke cell cycle arrest and senescence in part through the induction of DNA damage (19). One means by which the absence of VHL could lead to senescence is through increased amounts of such damage. We thus wished to determine whether cells deficient in VHL have higher levels of DNA damage when grown under atmospheric conditions, which might explain why they demonstrate an oxygen-dependent senescence response. To this end, we measured the levels of DNA damage in wild-type and VHL-null cells grown at 21% O_2 by immunoblotting for γH2AX and by denaturing comet assay. As shown in Fig. 2E, the loss of VHL had no effect on the levels of DNA damage in comparison to control cells, and the two populations showed equivalent induction of γH2AX staining following 4 Gy of IR. Accordingly, by comet assay, the two cell populations had similarly low levels of basal DNA damage and similar inductions of damage following 1, 2, or 4 Gy of IR (Fig. 2F). Thus, VHL-null cells do not senesce because they acquire more damage than wild-type cells when they are exposed to similar stresses. Instead, VHL loss evidently decreases the threshold of oxidative stress that is sufficient to induce senescence.

Senescence due to VHL loss is dependent on p27 at 21% O_2 but not under hypoxia. Young et al. recently observed that loss of VHL leads to an increase in the levels of the cell cycle regulatory protein p27 (Cdkn1B) (41). p27 inhibits the activation of cyclin E/cdk2 or cyclin D/cdk4 complexes that control cell cycle entry through phosphorylation of retinoblastoma protein (Rb) (5). According to Young et al., loss of VHL leads to a decrease in the expression of Skp2, which is involved in the degradation of p27, thereby resulting in an increase in stability of p27 and leading to cell cycle arrest and eventually senescence. Within the context of oxygen sensitivity, overexpression of p27 could explain why VHL-null cells are more sensitive to oxidative stress, as they would require less of a cooperating DNA damage signal to promote arrest.

To confirm these results and to determine how this pathway is affected by oxygen tension, we first measured the levels of p27 in heterogeneous populations of both wild-type and VHL-null cells at 21%, 10%, 5%, and 2% O_2 by immunoblotting. As shown in Fig. 3A, we also found that p27 was increased in VHL-null cells compared to wild-type cells under atmospheric conditions, to a level that was similar to that produced by treatment with the proteasome inhibitor MG132. In addition, this increase contributed to the induction of senescence, as knockdown of p27 increased the life span of these cells in normoxia (see Fig. S4 in the supplemental material).

Interestingly, however, under all of the oxygen tensions that we assayed, p27 remained at higher levels in the VHL-deficient cells than in wild-type cells (Fig. 3A), even under conditions in which both wild-type and VHL-null MEFs grow optimally (5% O_2). Since VHL has also been linked to regulation of the cell cycle through the transcriptional regulation of cyclin D1 (30) and to altered cell cycle dynamics (20), we also determined the effects on p27 in synchronized cells to rule out the possibility that the alterations in p27 levels were due to altered cell cycle profiles. We thus synchronized wild-type and VHL-null cells in 21% and 5% O_2 by serum starvation and then induced them to reenter the cell cycle by serum stimulation for periods of 4, 8, 12, or 24 h. Importantly, early-passage cells were used to ensure that the VHL-null cells in normoxia would still have the potential to reenter the cell cycle. All groups arrested to similar degrees as assessed by flow cytometry for propidium iodide staining (G_1 phase contents: wild type, 21% O_2, 98.24%; wild type, 5% O_2, 97.89%; VHL null, 21% O_2, 96.65%; and VHL null, 5% O_2, 97.46%). Following serum stimulation, p27 was more rapidly degraded in wild-type cells than in VHL-deficient cells under both oxygen conditions (Fig. 3B). However, there were negligible differences between higher and lower oxygen states with respect to p27 regulation.

We next wished to determine if other well-known cell cycle regulatory proteins might be altered under hypoxic conditions, which could explain why VHL loss induces senescence only under atmospheric oxygen conditions. To do so, we again utilized synchronized cells and measured the expression of various cell cycle regulatory proteins involved in the G_1/S transition, including cyclin A, cyclin D1, cyclin E, and p21. As shown in Fig. 3C, by 24 h of stimulation, all cell populations had similarly induced cyclin A and, to a lesser degree, cyclin E, suggesting that they had all equally started to enter S phase. This was confirmed by flow cytometry (S-phase contents: wild type, 21% O_2, 17.80%; wild type, 5% O_2, 12.98%; VHL null, 21% O_2, 12.18%; and VHL null, 5% O_2, 14.49%).

Interestingly, cyclin D1 revealed differences between the wild-type and VHL-null cells. While they all began to induce cyclin D1 by 8 h of stimulation, the wild-type cells expressed higher levels of cyclin D1 at both 21% and 5% O_2. This could be a result of the increased levels of p27 in the VHL-null cells, which at higher levels would decrease Rb activity that in turn regulates cyclin D1 expression by inhibiting E2F. This is in agreement with the decreased growth rate of VHL-null cells at all oxygen concentrations we observed (Fig. 1C). Notably, however, there was no difference in the induction of cyclin D1 in the VHL-null cells under 21% versus 5% oxygen, suggesting that altered cyclin D1 regulation does not rescue VHL-null cells at 5% O_2 and that VHL may not regulate cyclin D1 in mouse fibroblasts, as it has been reported to do in renal carcinoma cell lines (30).

However, we did find that cells maintained at 5% O_2 had significantly decreased levels of p21 (Cdkn1A) compared to cells at 21% O_2, regardless of VHL status. This is in agreement with the literature (28, 31), which demonstrates that oxidative stress from culturing cells at 21% oxygen induces a DNA damage response that activates p53 and subsequently p21. Since p21 and p27 both regulate the same critical step in cell

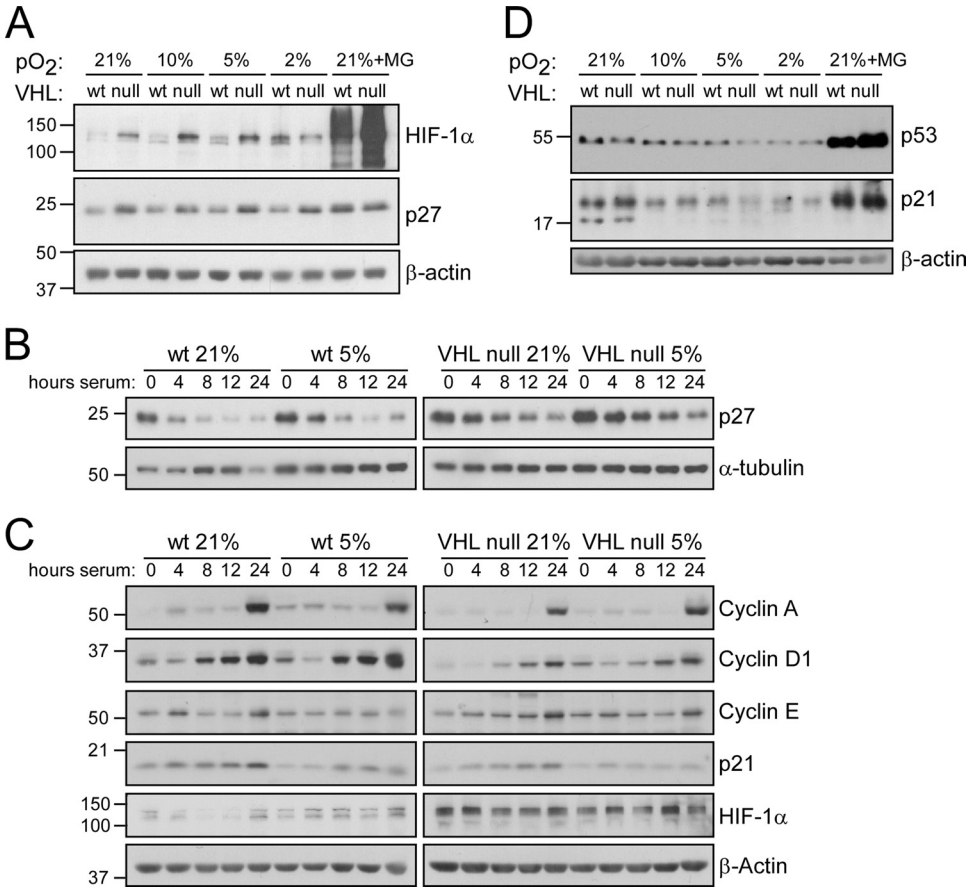

FIG. 3. p27 induction following VHL loss is not prevented under hypoxia, but p21 expression is attenuated. (A and D) Western analyses of wild-type or VHL-null MEFs grown at 21, 10, 5, or 2% O_2. MG, MG132. (B and C) Western analyses of serum-starved and stimulated wild-type or VHL-null MEFs in 21 or 5% O_2. To allow direct comparison, membranes were transferred in the same apparatus and developed on the same pieces of film.

cycle progression (inactivation of Rb), this observation suggests that the DNA damage pathway, together with increased p27 due to VHL inactivation, may promote premature senescence. To assess the levels of p53 in these cells as a function of the oxygen concentration, we again analyzed lysates from asynchronous populations that were maintained at various oxygen levels. Indeed, we found that p53 levels were highest in cells maintained at 21% oxygen and decreased as cells were grown at reduced levels of oxygen (Fig. 3D). Additionally, p21 levels correlated well with p53 levels, showing the highest levels at 21% oxygen and the lowest at 2% oxygen. VHL status, however, did not have an effect on either p53 or p21 levels. Together, these data suggest that the p53 pathway might contribute to the senescence response in VHL-deficient cells in a manner that would confer oxygen dependence.

Senescence due to VHL loss is dependent on p53. To directly test whether p53 is required for senescence following VHL loss, we stably inactivated p53 using a lentivirus-mediated shRNA and then assessed the effects of VHL loss on proliferation and induction of senescence at atmospheric oxygen levels. As shown in Fig. 4A, the shRNA to p53 led to a significant reduction of p53 expression and serine 18 phosphorylation following treatment with doxorubicin in the parental cells. These cells were subsequently treated with adenovirus to inactivate VHL. As shown in Fig. 4B and C, loss of VHL led to stabilization of HIF-1α and increased expression of Glut1, whereas knockdown of p53 led to an expected decrease of p21 mRNA and protein levels. Interestingly, there was a corresponding increase in basal levels of γH2AX staining in the p53 knockdown cells, consistent with an accumulation of unrepaired damage in these cells. In the absence of VHL, p27 was again increased, and while overall levels seemed to increase in the p53 knockdown cells, these levels were further augmented with VHL inactivation.

When we compared the growth characteristics of these cells, we observed again that loss of VHL alone resulted in an increase in senescence compared to wild-type cells (Fig. 4D and E). In contrast, p53 loss led to immortalization of both the wild-type and VHL-null cells; these cells did not display characteristics of senescence. Thus, p53 is required for induction of senescence due to VHL loss.

VHL loss does not lead to senescence in primary renal epithelial cells when they are cultured at physiological oxygen tensions. In light of our observation that oxygen levels have a considerable impact on the fate of cells that lose VHL, we sought to determine the biological significance of these findings. VHL loss is characteristic of a number of tumor phenotypes, including CNS and retinal hemangioblastomas, pheo-

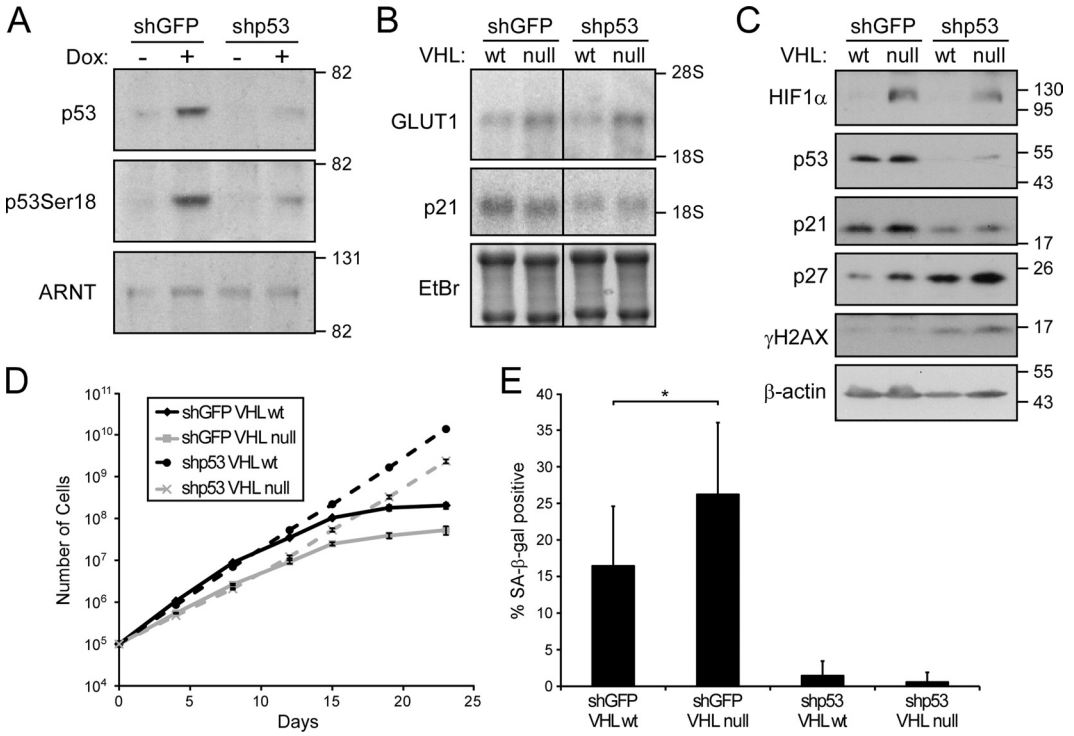

FIG. 4. Inactivation of p53 alleviates senescence following VHL loss. (A) Western analysis of wild-type MEFs expressing shRNA to GFP or p53 and treated with doxorubicin (Dox) as indicated. (B) Northern analysis of wild-type or VHL-deficient MEFs expressing shRNA to GFP or p53. EtBr, ethidium bromide. (C) Western analysis of cells as for panel B. (D) Proliferation profiles of cells as in panel B. (E) Quantification of SA-β-Gal staining of cells in panel D at day 23 (*, $P = 0.01$). The error bars represent standard deviations.

chromocytomas, and, in particular, clear-cell renal cell carcinomas. Within the kidney, the partial pressure of oxygen varies considerably, reaching as low as 10 to 20 mm Hg (equivalent to 1.5 to 3% O_2) in the inner medulla to as high as 50 mm Hg (~7% O_2) in the far outer cortex (1, 18). As the cells of origin for VHL-deficient CCRCC are thought to be the proximal tubule (24) or distal tubule (21) epithelial cells, which are primarily restricted to the cortical region, we focused our attention on that region.

We used pimonidazole and Glut1 staining to confirm the oxygen tensions of normal kidneys and peanut agglutinin (PNA) and *G. simplicifolia* II (GSII) to locate proximal tubule cells within the oxygen gradient (32). Pimonidazole and Glut1 staining of normal kidneys was mainly restricted to the inner and outer medulla, with Glut1 entering the cortic-medullary boundary (see Fig. S5 and S6 in the supplemental material), which is consistent with the progressive stabilization of HIF-1α at levels of oxygen below 5 to 6% (13). Proximal tubule cells were found to border the Glut1-positive region, essentially demarcating the renal cortex from the medulla, suggesting that tubular epithelial cells reside in an environment that is roughly 4 to 7% oxygen. This is in agreement with previous studies, as well as with our own OxyLite electrode measurements (data not shown).

To assess the effect of VHL loss on renal tubule epithelial cells, we made use of a proximal-tubule-specific *Vhlh* knockout mouse that was recently reported (29). PEPCK-CRE VHL mice develop microscopic and macroscopic tubular cysts at ages greater than 1 year. Until that time, VHL deficiency does not manifest an overt phenotype *in vivo* in the proximal tubules. *A priori*, this suggests that loss of VHL alone does not lead to senescence *in vivo*.

We isolated PTECs from PEPCK-CRE $VHL^{f/f}$ and PEPCK-CRE $VHL^{f/+}$ mice to assess the effects of the oxygen concentration on their fate. PCR analysis performed on genomic DNA revealed inactivation of *Vhlh* in both genotypes that was specific to the renal epithelial cells (Fig. 5A; note the presence of the recombined *1-lox* allele in DNA from the PTECs from both animals, but not in tail DNA). We next cultured these cells in either 21% O_2 or 5% O_2, similar to the oxygen levels they experience *in vivo*. Strikingly, after only 3 days in culture, we observed that the PTECs derived from the PEPCK-CRE $VHL^{f/f}$ mice exhibited a significant number of senescent cells, which was strictly dependent on the oxygen concentration (Fig. 5B). At 21% O_2, there were 14.9% ± 2.0% SA-β-Gal-positive cells, while at 5% O_2 there were less than 1% (0.5% ± 0.9%) positive cells (Fig. 5C). At the same time, the VHL-heterozygous cells contained essentially no senescent cells at either oxygen concentration (0.6% ± 0.3% at 21% O_2 and 0.5% ± 1.0% at 5% O_2). We also stained these cells for the renal epithelial markers PNA and GSII and found that the senescent cells were in fact of epithelial origin and not contaminating cells in the culture (Fig. 5C). These data confirm our findings in MEFs and demonstrate that loss of VHL in renal epithelial cells leads to senescence only when the cells are challenged with additional oxidative stress.

Paraquat treatment can induce senescence in VHL-deficient renal proximal tubules *in vivo*. Together, our *in vitro* data

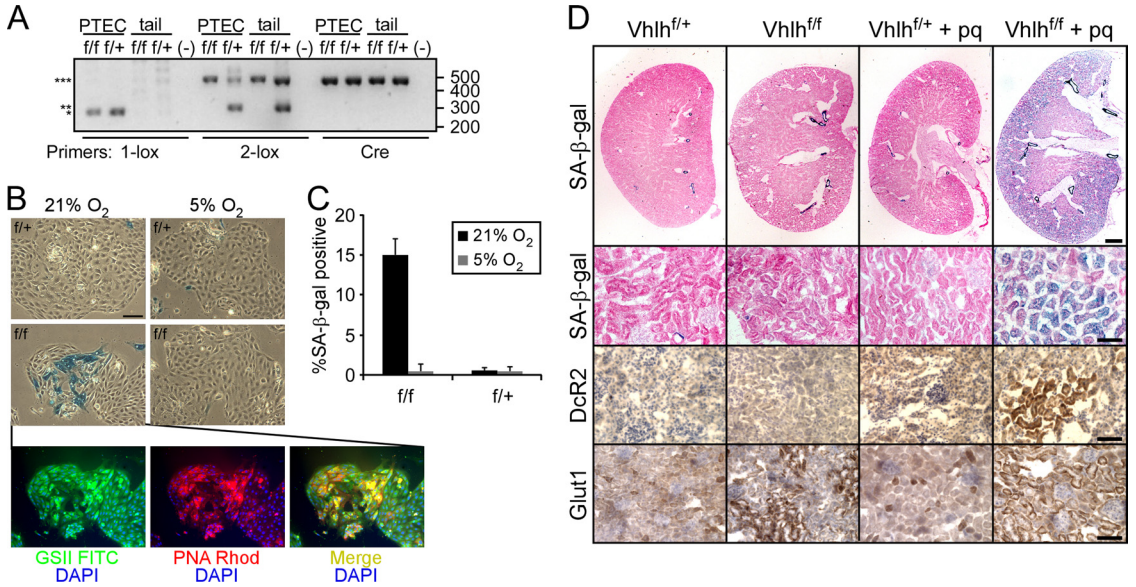

FIG. 5. Normal kidney oxygenation inhibits senescence in primary renal tubule epithelial cells. (A) Genomic analysis of *Vhlh* status in PTECs and tail DNA from PEPCK-CRE $VHL^{f/f}$ and $VHL^{f/+}$ mice. 1-lox primers amplify the recombined allele (*); 2-lox primers amplify the nonrecombined (***) and wild-type (**) alleles. Sizes are indicated in base pairs on the right. (B) SA-β-Gal staining of PEPCK-CRE $VHL^{f/f}$ and $VHL^{f/+}$ PTECs grown at either 21% or 5% O_2 for 3 days and lectin staining of the PEPCK-CRE $VHL^{f/f}$ PTECs at 21%. Bar = 100 μm. DAPI, 4′,6-diamidino-2-phenylindole; Rhod, rhodamine. (C) Quantification of SA-β-Gal staining of cells in panel C ($P < 0.00024$ for f/f at 21% versus 5% or f/+ at 21%). (D) SA-β-Gal, DcR2, and Glut1 staining of PEPCK-CRE $VHL^{f/+}$ or $VHL^{f/f}$ kidneys 4 weeks after treatment with paraquat (pq). Bar = 500 μm (upper row) or 50 μm (lower rows).

suggest that VHL deficiency leads to a significant sensitization to oxidative stress that can manifest itself in the induction of senescence. To determine if this model holds true *in vivo*, we sought to induce robust oxidative stress to the renal proximal tubes of the PEPCK-CRE VHL animals through the use of paraquat, a potent oxidizing agent to which the kidney is particularly sensitive (23, 27, 36, 40). Following treatment with 10 mg/kg of paraquat dichloride, animals were monitored and sacrificed after 4 weeks, and their kidneys were sectioned and stained for SA-β-Gal and for the senescence marker DcR2. As seen in the representative kidneys in Fig. 5D, we found that paraquat treatment of only the VHL-null kidneys resulted in significant induction of senescence throughout the renal cortex, as measured by both senescence markers. Importantly, this excluded the renal medulla, where VHL was not inactivated. In contrast, the untreated PEPCK-CRE $VHL^{f/+}$, PEPCK-CRE $VHL^{f/f}$, and treated PEPCK-CRE $VHL^{f/+}$ animals showed little evidence of senescence (although all kidneys, regardless of genotype or treatment, showed some nonspecific staining of smooth muscle in arcuate or renal arteries). In addition, we confirmed the genotypes of these animals by staining for Glut1 and found that both treated and untreated PEPCK-CRE $VHL^{f/f}$ animals demonstrated positive staining. Cumulatively, we observed senescence in the kidneys of 57% ($n = 7$) of the treated PEPCK-CRE $VHL^{f/f}$ animals compared to none of the untreated ($n = 9$), treated PEPCK-CRE $VHL^{f/+}$ ($n = 9$), or untreated PEPCK-CRE $VHL^{f/+}$ ($n = 9$) animals.

DISCUSSION

In this report, we demonstrate that loss of VHL can lead to induction of senescence in mouse embryo fibroblasts and in primary renal epithelial cells in atmospheric oxygen but not when cells are maintained at physiological oxygen levels. This effect depends on the modulation of oxidative stress, as senescence can be induced at physiological pO_2 by exposing cells to ionizing radiation or H_2O_2. In addition, we identified a mechanism for this oxygen dependence, i.e., induction of a p53-dependent signaling pathway, suggesting that VHL loss, by increasing levels of p27, cooperates with stress-induced p53 to promote senescence. Significantly, we also show that senescence occurs in VHL-deficient renal epithelial cells *in vivo* in an oxidative-stress-dependent manner and that *in vivo* oxygen levels in the kidney are sufficient to suppress this response in the absence of exogenous stress. Together, these data indicate that VHL loss makes cells more sensitive to senescence-inducing stresses but that VHL loss *per se* is a tolerated event *in vivo*.

Mechanistically, we found that these effects are independent of the HIF pathway. We have recently published evidence that the VHL target HIF-1α also plays a role in the regulation of senescence. HIF-1α can impair the onset of senescence through transcriptional activation of various target genes, such as *MIF* (38) and *TERT* (2). Although TERT expression is not generally involved in senescence in mouse cells, overexpression of MIF can prolong the life span of MEFs through inhibition of p53 (12). Thus, inactivation of VHL, which leads to HIF-1α activity and MIF upregulation, could be hypothesized to inhibit, not induce, senescence. Our current data, however, suggest that the prosenescence effects of VHL loss outweigh the antisenescence effects downstream of HIF-1α. In keeping with this concept, we found that senescence induced by VHL loss was independent of HIF-1α and HIF-2α and that in fact, com-

bined inactivation of both VHL and HIF-1α led to an exacerbated phenotype (see Fig. S7 in the supplemental material).

Instead, VHL loss appears to induce senescence by modulating p27, which in turn lowers the levels of oxidative stress that a cell can withstand. Subsequent stress-induced p53 activation leads to senescence of VHL-deficient cells. In support of this, inhibition of either p27 or p53 expression is sufficient to inhibit VHL loss-induced senescence. In this regard, our findings are seemingly at odds with the report by Young et al., which suggested that VHL loss leads to senescence in a p53-independent manner (41). One potential explanation for our differing observations is experimental design. In our experiments, we maintained our cells under physiological oxygen conditions during all manipulations and then exposed them to the appropriate oxygen levels, as indicated. For example, to inactivate p53, we infected and selected the cells in a low-oxygen environment and then inactivated VHL in the same environment. Importantly, this treatment preserved the replicative potential of the cells until the initiation of the experiment. In contrast, when we performed these same manipulations under atmospheric oxygen conditions prior to initiation of the experiment, we obtained a different result (see Fig. S8 in the supplemental material). In this case, it appeared that inactivation of p53 was insufficient to alleviate senescence due to VHL loss. Therefore, our data indicate that oxidative stress due to culturing primary cells in what is effectively hyperoxia during the experimental preparation may lead to opposing conclusions about the role of p53 in VHL loss-induced senescence.

Collectively, our findings imply that certain *in vivo* oxygen tensions, for example, the moderately low-oxygen environment found in the renal cortex, may allow tolerance of VHL loss and allow cells to progress further toward a transformed state. This hypothesis is corroborated by the viability of two distinct renal-epithelial-specific VHL knockout mice (9, 29). Aside from the development of renal cysts at advanced ages, both of these models lack overt renal phenotypes independent of other alterations. It is unlikely that senescent tubule epithelial cells would allow normal renal development and function, given the dramatic changes in gene expression and behavior of senescent cells, particularly as in both models inactivation of VHL occurs during embryogenesis. While it is possible that senescent VHL-deficient cells would be cleared (39), this also seems unlikely, given the persistence of VHL-deficient cells in aged animals. In agreement with this, we were unable to detect senescent cells within the proximal tubes of the kidneys of a large number of the PEPCK-CRE $VHL^{f/f}$ animals of various ages. While this observation is again in contrast with the results of Young et al., differences in our experimental models (including mouse strains, tissue specificities of CRE expression, and methods of activation of CRE) may explain these differences. Thus, in the renal proximal tubule at least, oxygen tensions appear to be permissive for the persistence of VHL-deficient cells.

Interestingly, the model we used for kidney-specific inactivation of VHL (PEPCK-driven CRE recombinase), also leads to inactivation in portions of the liver, an organ that also commonly displays phenotypes associated with von Hippel-Lindau disease. This allowed us also to assess the effects of VHL loss in the liver in the same animals. In agreement with our findings in the kidney, we also did not observe senescence in the periportal regions of the liver (data not shown), where PEPCK is expressed and where oxygen concentrations can range from 5.9 to 6.6% O_2 (14). This further supports the concept that where *in vivo* manifestations of VHL disease occur, senescence may not be occurring due to a permissive oxygen environment.

VHL-deficient renal cell carcinomas are notoriously difficult to treat, being refractory to standard chemo- and radiotherapy regimens. This is in spite of the highly vascular nature of these tumors, which results from hyperactivation of the HIF pathways that regulate angiogenesis. Here, we have shown that VHL-deficient primary cells have increased sensitivity to oxidative stress, a phenotype they would have to overcome during the transformation process. It is tempting to hypothesize that the mode by which VHL-deficient cells overcome this sensitivity is related to their resistance to common therapies that rely on robust DNA damage to induce cell death. In this light, our data establish a framework from which to study the further genetic abnormalities that might turn a VHL-deficient renal epithelial cell into an initiator of renal carcinoma.

ACKNOWLEDGMENTS

This work was funded by NIH CA088480.

We thank Alejandro Sweet-Cordero for the shRNA to p53; Pauline Chu for assistance with histology; and Barbara Bedogni, Kevin Bennewith, and Erinn Rankin for critical review of the manuscript.

REFERENCES

1. **Aukland, K., and J. Krog.** 1960. Renal oxygen tension. Nature **188:**671.
2. **Bell, E. L., T. A. Klimova, J. Eisenbart, P. T. Schumacker, and N. S. Chandel.** 2007. Mitochondrial reactive oxygen species trigger hypoxia-inducible factor-dependent extension of the replicative life span during hypoxia. Mol. Cell. Biol. **27:**5737–5745.
3. **Bertout, J. A., S. A. Patel, and M. C. Simon.** 2008. The impact of O2 availability on human cancer. Nat. Rev. Cancer **8:**967–975.
4. **Chen, Z., L. C. Trotman, D. Shaffer, H. K. Lin, Z. A. Dotan, M. Niki, J. A. Koutcher, H. I. Scher, T. Ludwig, W. Gerald, C. Cordon-Cardo, and P. P. Pandolfi.** 2005. Crucial role of p53-dependent cellular senescence in suppression of Pten-deficient tumorigenesis. Nature **436:**725–730.
5. **Chu, I. M., L. Hengst, and J. M. Slingerland.** 2008. The Cdk inhibitor p27 in human cancer: prognostic potential and relevance to anticancer therapy. Nat. Rev. Cancer. **8:**253–267.
6. **Courtois-Cox, S., S. M. Genther Williams, E. E. Reczek, B. W. Johnson, L. T. McGillicuddy, C. M. Johannessen, P. E. Hollstein, M. MacCollin, and K. Cichowski.** 2006. A negative feedback signaling network underlies oncogene-induced senescence. Cancer Cell **10:**459–472.
7. **Dimri, G. P., X. Lee, G. Basile, M. Acosta, G. Scott, C. Roskelley, E. E. Medrano, M. Linskens, I. Rubelj, O. Pereira-Smith, et al.** 1995. A biomarker that identifies senescent human cells in culture and in aging skin in vivo. Proc. Natl. Acad. Sci. U. S. A. **92:**9363–9367.
8. **Dorie, M. J., M. S. Kovacs, E. C. Gabalski, M. Adam, Q. T. Le, D. A. Bloch, H. A. Pinto, D. J. Terris, and J. M. Brown.** 1999. DNA damage measured by the comet assay in head and neck cancer patients treated with tirapazamine. Neoplasia **1:**461–467.
9. **Frew, I. J., C. R. Thoma, S. Georgiev, A. Minola, M. Hitz, M. Montani, H. Moch, and W. Krek.** 2008. pVHL and PTEN tumour suppressor proteins cooperatively suppress kidney cyst formation. EMBO J. **27:**1747–1757.
10. **Fridovich, I.** 1998. Oxygen toxicity: a radical explanation. J. Exp. Biol. **201:** 1203–1209.
11. **Haase, V. H., J. N. Glickman, M. Socolovsky, and R. Jaenisch.** 2001. Vascular tumors in livers with targeted inactivation of the von Hippel-Lindau tumor suppressor. Proc. Natl. Acad. Sci. U. S. A. **98:**1583–1588.
12. **Hudson, J. D., M. A. Shoaibi, R. Maestro, A. Carnero, G. J. Hannon, and D. H. Beach.** 1999. A proinflammatory cytokine inhibits p53 tumor suppressor activity. J. Exp. Med. **190:**1375–1382.
13. **Jiang, B. H., G. L. Semenza, C. Bauer, and H. H. Marti.** 1996. Hypoxia-inducible factor 1 levels vary exponentially over a physiologically relevant range of O2 tension. Am. J. Physiol. **271:**C1172–C1180.
14. **Jungermann, K., and T. Kietzmann.** 2000. Oxygen: modulator of metabolic zonation and disease of the liver. Hepatology **31:**255–260.
15. **Kaelin, W. G., Jr.** 2008. The von Hippel-Lindau tumour suppressor protein: O2 sensing and cancer. Nat. Rev. Cancer **8:**865–873.

16. **Kaelin, W. G., Jr., and P. J. Ratcliffe.** 2008. Oxygen sensing by metazoans: the central role of the HIF hydroxylase pathway. Mol. Cell **30:**393–402.
17. **Lee, A. C., B. E. Fenster, H. Ito, K. Takeda, N. S. Bae, T. Hirai, Z. X. Yu, V. J. Ferrans, B. H. Howard, and T. Finkel.** 1999. Ras proteins induce senescence by altering the intracellular levels of reactive oxygen species. J. Biol. Chem. **274:**7936–7940.
18. **Leichtweiss, H. P., D. W. Lubbers, C. Weiss, H. Baumgartl, and W. Reschke.** 1969. The oxygen supply of the rat kidney: measurements of intrarenal pO2. Pflugers Arch. **309:**328–349.
19. **Li, H., J. R. Mitchell, and P. Hasty.** 2008. DNA double-strand breaks: a potential causative factor for mammalian aging? Mech. Ageing Dev. **129:** 416–424.
20. **Mack, F. A., J. H. Patel, M. P. Biju, V. H. Haase, and M. C. Simon.** 2005. Decreased growth of *Vhl*$^{-/-}$ fibrosarcomas is associated with elevated levels of cyclin kinase inhibitors p21 and p27. Mol. Cell. Biol. **25:**4565–4578.
21. **Mandriota, S. J., K. J. Turner, D. R. Davies, P. G. Murray, N. V. Morgan, H. M. Sowter, C. C. Wykoff, E. R. Maher, A. L. Harris, P. J. Ratcliffe, and P. H. Maxwell.** 2002. HIF activation identifies early lesions in VHL kidneys: evidence for site-specific tumor suppressor function in the nephron. Cancer Cell **1:**459–468.
22. **Michaloglou, C., L. C. Vredeveld, M. S. Soengas, C. Denoyelle, T. Kuilman, C. M. van der Horst, D. M. Majoor, J. W. Shay, W. J. Mooi, and D. S. Peeper.** 2005. BRAFE600-associated senescence-like cell cycle arrest of human naevi. Nature **436:**720–724.
23. **Mølck, A. M., and C. Friis.** 1997. The cytotoxic effect of paraquat to isolated renal proximal tubular segments from rabbits. Toxicology **122:**123–132.
24. **Motzer, R. J., N. H. Bander, and D. M. Nanus.** 1996. Renal-cell carcinoma. N. Engl. J. Med. **335:**865–875.
25. **Packer, L., and K. Fuehr.** 1977. Low oxygen concentration extends the lifespan of cultured human diploid cells. Nature **267:**423–425.
26. **Parrinello, S., E. Samper, A. Krtolica, J. Goldstein, S. Melov, and J. Campisi.** 2003. Oxygen sensitivity severely limits the replicative lifespan of murine fibroblasts. Nat. Cell Biol. **5:**741–747.
27. **Pond, S. M., L. P. Rivory, E. C. Hampson, and M. S. Roberts.** 1993. Kinetics of toxic doses of paraquat and the effects of hemoperfusion in the dog. J. Toxicol. Clin. Toxicol. **31:**229–246.
28. **Poulios, E., I. P. Trougakos, N. Chondrogianni, and E. S. Gonos.** 2007. Exposure of human diploid fibroblasts to hypoxia extends proliferative life span. Ann. N. Y. Acad. Sci. **1119:**9–19.
29. **Rankin, E. B., J. E. Tomaszewski, and V. H. Haase.** 2006. Renal cyst development in mice with conditional inactivation of the von Hippel-Lindau tumor suppressor. Cancer Res. **66:**2576–2583.
30. **Raval, R. R., K. W. Lau, M. G. Tran, H. M. Sowter, S. J. Mandriota, J. L. Li, C. W. Pugh, P. H. Maxwell, A. L. Harris, and P. J. Ratcliffe.** 2005. Contrasting properties of hypoxia-inducible factor 1 (HIF-1) and HIF-2 in von Hippel-Lindau-associated renal cell carcinoma. Mol. Cell. Biol. **25:**5675–5686.
31. **Roy, S., S. Khanna, A. A. Bickerstaff, S. V. Subramanian, M. Atalay, M. Bierl, S. Pendyala, D. Levy, N. Sharma, M. Venojarvi, A. Strauch, C. G. Orosz, and C. K. Sen.** 2003. Oxygen sensing by primary cardiac fibroblasts: a key role of p21(Waf1/Cip1/Sdi1). Circ. Res. **92:**264–271.
32. **Schulte, B. A., and S. S. Spicer.** 1983. Histochemical evaluation of mouse and rat kidneys with lectin-horseradish peroxidase conjugates. Am. J. Anat. **168:** 345–362.
33. **Serrano, M., A. W. Lin, M. E. McCurrach, D. Beach, and S. W. Lowe.** 1997. Oncogenic ras provokes premature cell senescence associated with accumulation of p53 and p16INK4a. Cell **88:**593–602.
34. **Taub, M., and G. Sato.** 1980. Growth of functional primary cultures of kidney epithelial cells in defined medium. J. Cell. Physiol. **105:**369–378.
35. **Vaupel, P., F. Kallinowski, and P. Okunieff.** 1989. Blood flow, oxygen and nutrient supply, and metabolic microenvironment of human tumors: a review. Cancer Res. **49:**6449–6465.
36. **Vaziri, N. D., R. L. Ness, R. D. Fairshter, W. R. Smith, and S. M. Rosen.** 1979. Nephrotoxicity of paraquat in man. Arch. Intern. Med. **139:**172–174.
37. **von Zglinicki, T., G. Saretzki, W. Docke, and C. Lotze.** 1995. Mild hyperoxia shortens telomeres and inhibits proliferation of fibroblasts: a model for senescence? Exp. Cell Res. **220:**186–193.
38. **Welford, S. M., B. Bedogni, K. Gradin, L. Poellinger, M. Broome Powell, and A. J. Giaccia.** 2006. HIF1alpha delays premature senescence through the activation of MIF. Genes Dev. **20:**3366–3371.
39. **Xue, W., L. Zender, C. Miething, R. A. Dickins, E. Hernando, V. Krizhanovsky, C. Cordon-Cardo, and S. W. Lowe.** 2007. Senescence and tumour clearance is triggered by p53 restoration in murine liver carcinomas. Nature **445:**656–660.
40. **Yonemitsu, K.** 1986. Pharmacokinetic profile of paraquat following intravenous administration to the rabbit. Forensic Sci. Int. **32:**33–42.
41. **Young, A. P., S. Schlisio, Y. A. Minamishima, Q. Zhang, L. Li, C. Grisanzio, S. Signoretti, and W. G. Kaelin, Jr.** 2008. VHL loss actuates a HIF-independent senescence programme mediated by Rb and p400. Nat. Cell Biol. **10:**361–369.